Turkish Journal of Electrical Engineering & Computer Sciences

http://journals.tubitak.gov.tr/elektrik/

Research Article

Turk J Elec Eng & Comp Sci
(2019) 27: 921 – 938

doi:10.3906/elk-1805-193

Hybrid control of five-phase permanent magnet synchronous machine using space vector modulation

Djamel DIFI[1,*], **Khaled HALBAOUI**[2], **Djamel BOUKHETALA**[1]
[1]Process Control Laboratory, National Polytechnic School, Algiers, Algeria
[2]Power Electronics Laboratory, Nuclear Research Centre of Brine CRNB, Djelfa, Algeria

Received: 28.05.2018 • **Accepted/Published Online:** 06.12.2018 • **Final Version:** 22.03.2019

Abstract: This paper aims to study the hybrid control of a five-phase permanent-magnet synchronous machine improved by the space vector modulation (SVM) technique. The torque ripples and currents will therefore be reduced. This control is based on the theory of hybrid dynamic systems (HDS), its discrete component is the voltage inverter which has a finite number of states controlling the continuous component that represents the machine. The results of the simulation made on MATLAB/Simulink are presented and discussed in order to check the performance of the strategy of the studied control. They show, in particular, the main advantages of this control manifesting the good dynamic of the electromagnetic torque and the robustness against the parametric variations.

Key words: Hybrid dynamic systems (HDS), hybrid control, space vector modulation technique, multiphase machine, five-phase permanent-magnet synchronous machine, robust control

1. Introduction

In recent years, multiphase machine application has been widely promoted by researchers in many fields such as electronic vehicles, railway traction, all-electric ships, electric aircraft, and wind power generation systems [1–7]. The raising interest in this type of machines is the result of the advantages it enjoys when compared to the three-phase [1, 3–5, 7–10], in terms of the performance they provide, such as better fault tolerance, higher torque density, less torque pulsation, drive noise characteristic improvement, and a smaller sum in ratting per inverter leg [1–7, 9–11]; as well as the increase of digital-calculators power [12, 13] , and advances in the field of electronic power [6, 14].

These industrial applications require torque control with high dynamic performance, good steady-state accuracy, and robustness to different disturbances. In recent years, several techniques have been developed to enable this performance. The vector control makes it possible to have a dynamic close to that of the DC machine; however, this control structure requires precise parameters of the machine [15–17], which in turn requires a good identification of the parameters. Consequently, it is necessary to use a robust control algorithm to guarantee an acceptable level of decoupling and performance [4].

The conventional direct torque control (DTC) strategy is a solution for the problems of the vector control; it uses an enticing approach with its efficiency and simplicity of implementation [16–18]. In this technique, the inverter commutations are obtained from the output information of the two hysteresis regulators (torque, flux) and the position of the stator flux [3, 6, 14, 16, 17, 19–21]. Because of these regulators, the frequency of the

*Correspondence: d.difi@yahoo.fr

power switch control is not constant, which causes a harmonic-rich spectral content that increases the losses in the machine [3, 6, 16–21]. In order to overcome this problem, this method is improved by eliminating the hysteresis regulators and the vector selection table. This new strategy is based on the PI regulators and the SVM technique, in which the inverter operates at a constant frequency, and the SVM is applied to the output vector of the control [6, 16, 18–21]. This technique (synchronous DTC) offers an alternative solution avoiding the disadvantages of the conventional DTC [6, 16, 18–21].

The hybrid control is a control that maintains the velocity of the DTC control and it is the best in terms of amplitude of the torque oscillations. This control allows the machine torque to be controlled directly at the level of the inverter commutations, which reduces the complexity of the algorithm. In addition, this control does not need any observers or current regulators [22–27]. This hybrid control, like the DTC control, does not require speed control, and it can be found in many applications, such as railroad traction, machine tools, and recently, electric vehicles. However, the speed of machine can be regulated through an external loop independent of the hybrid control. The output of its regulator is the electromagnetic reference torque

This type of control based on an hybrid dynamic systems (HDS) class model, i.e. modeling includes at the same time continuous and discrete variables [28–33], in the sense that the "discrete" behavior of the voltage inverter and the "continuous" behavior of the machine are taken into account in a unified manner during the modeling process. This control is applied to a large category of systems proposed in [22–27] and recently to multicellular converters [31, 34–37]. This diversity in application fields is based on a unique principle of the prediction phenomenon. This principle can be summarized in the following five steps:

- Determination of a general model of the behavior of the set energy modulator continuous process. It takes into account the continuous and discrete variables of the system.

$$\frac{dx}{dt} = f(x(t), u_j(t)); j \in 1, 2, ..., n. \tag{1}$$

- The integration of Eq. (1) by the Euler method over a short time interval T.

$$x(t+T) = x(t) + Tf(x(t), u_j(t)). \tag{2}$$

- Searching for the linearity domain in which the trajectories in the state space are rectilinear. This constraint implies the determination of the maximum decision time T_{max} and a minimum time T_{min}, the latter is a function of temporal execution constraints, material, and computing capacity.

- From a measured state x(t), we determine the possible directions d_j in the state space relative to the different switching states u_j.

$$d_j = x(t+T) - x(t) = Tf(x(t), u_j(t)). \tag{3}$$

- Choosing the closest direction to the reference state, we then apply the corresponding configuration to the chosen direction during an optimized time by respecting the constraint of linearity of the trajectories.

  In this favorable context to the development of new methods, the work presented in this paper aimed to improve and apply this hybrid approach for the torque control of the five-phase machines, while benefiting from the SVM technique. This improvement was based on maintaining the first four stages and replacing the last step with the following steps

- Determining the sector formed by d_i and d_{i+1} containing the vector d_{ref}.
- Decomposing the vector d_{ref} following the two vectors d_i and d_{i+1} delimiting the sector i.
- Elaborating the control sequences of the inverter switches.

As a result, the functioning of the system can be improved, whereas the ripples of the torque and currents will therefore be reduced. The obtained model was simulated using MATLAB/Simulink, and the results of this simulation are presented and compared with that of the vector control to check the performance of this control.

2. Proposed control principle

Figure 1 shows the principle of the control proposed in this paper. The currents i_α and i_β are calculated using the measured value of the stator phase currents. A hybrid model makes it possible to determine the components of different direction vectors d_j for the various switches of the inverter S_j. The block of the transformation of Park permits to transform the reference currents i_{dref} and i_{qref} into two sinusoidal currents $i_{\alpha ref}$ and $i_{\beta ref}$ which are applied to the inputs of the calculation block of the desired direction d_{ref}, this reference vector is found in a sector formed by d_i and d_{i+1} and then, an optimization procedure was carried out for selecting these two directions and their duration of application t_i and t_{i+1} to obtain a vector closest to the desired direction.

3. Modeling of five-phase permanent-magnet synchronous machine and its converter

3.1. Mathematical model of the five-phase permanent-magnet synchronous machine

In order to obtain a simpler formulation and reduce the complexity of the machine model, the establishment of its mathematical model will be developed on the basis of the following assumptions [38]:

- The effects of skin, shock absorbers, saturation, and variation of reluctance of the magnetic circuit are neglected.
- The EMF induced in the stator windings are solely due to the rotor magnets which have a shape that is due only to the magnets and the structure of the windings. Armature reaction magnetic (due to stator currents) does not change the form of the EMF.
- The phases are the same and offset by an $\alpha = \frac{2\pi}{5}$.

  The voltage equations of a five-phase permanent-magnet synchronous machine (PMSM) are given in [9, 10]:

$$[V] = [R][I] + [L]\frac{1}{dt}[I] + [E], \tag{4}$$

  where $[V]$ is the voltage vector, $[I]$ the current vector, $[E]$ the back electromotive force (EMF) vector, $[L]$ the inductance matrix, and $[R]$ the stator resistance matrix.

The five-phase machine is equivalent to three fictitious machines magnetically decoupled and mechanically coupled.

These three fictitious machines are called respectively the main machine, secondary machine, and homopolar machine[12].

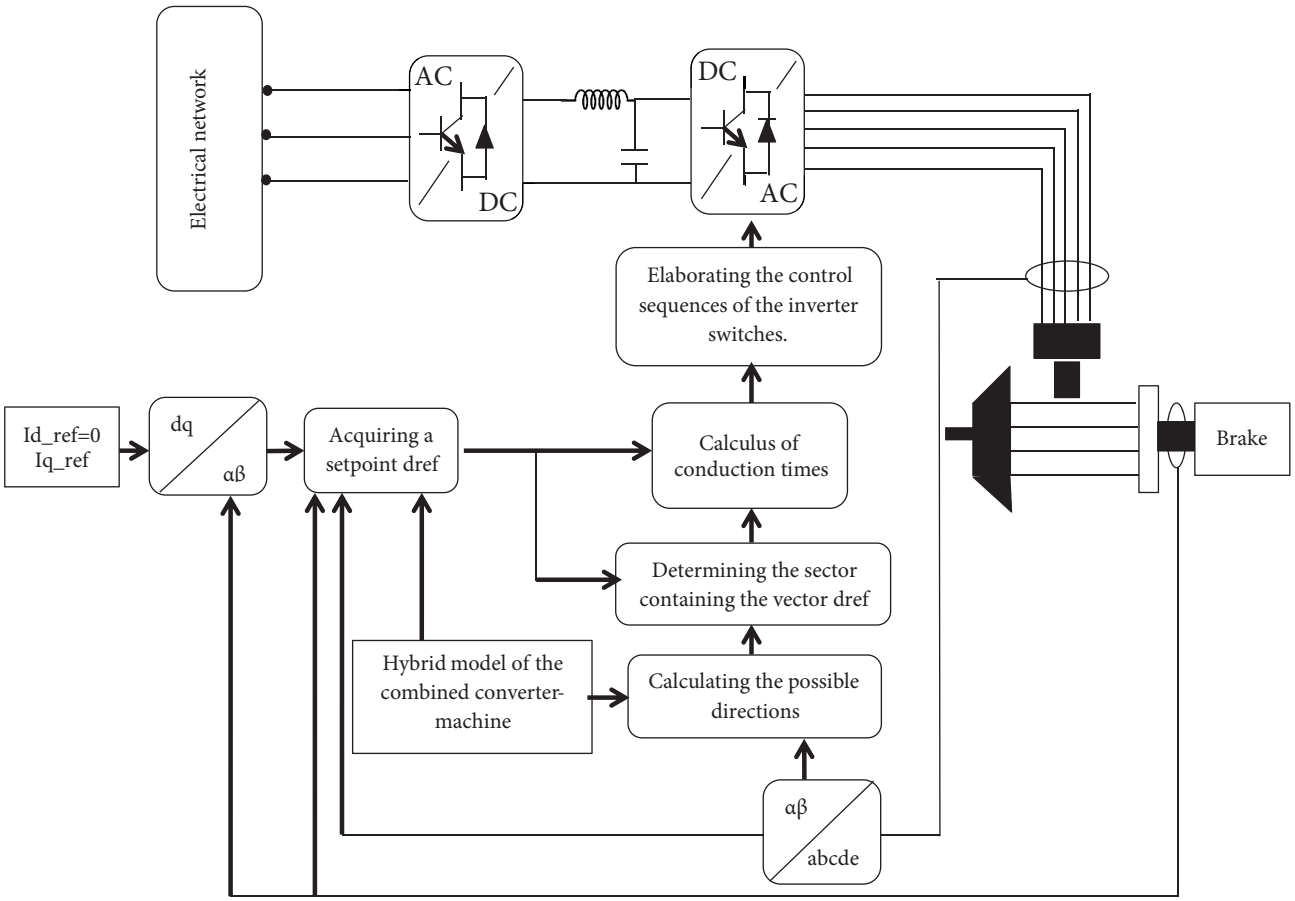

Figure 1. Principle of the hybrid control.

The transition from the natural base to the fictitious base is done through the intermediary of the Clarke transformation, which ensures the decoupling of the phases. The two transformation matrices in each plane are:

$$[C_p] = \begin{bmatrix} 1 & cos(\frac{2\pi}{5}) & cos(\frac{4\pi}{5}) & cos(\frac{6\pi}{5}) & cos(\frac{8\pi}{5}) \\ 0 & sin(\frac{2\pi}{5}) & sin(\frac{4\pi}{5}) & sin(\frac{6\pi}{5}) & sin(\frac{8\pi}{5}) \end{bmatrix}, \tag{5}$$

$$[C_s] = \begin{bmatrix} 1 & cos(\frac{6\pi}{5}) & cos(\frac{2\pi}{5}) & cos(\frac{8\pi}{5}) & cos(\frac{4\pi}{5}) \\ 0 & sin(\frac{6\pi}{5}) & sin(\frac{2\pi}{5}) & sin(\frac{8\pi}{5}) & sin(\frac{4\pi}{5}) \end{bmatrix}. \tag{6}$$

The electrical model of each fictitious machine can be put in the following matrix forms:

- Main machine:

$$\frac{d}{dt}\begin{bmatrix} I_{\alpha p} \\ I_{\beta p} \end{bmatrix} = \begin{bmatrix} \frac{-R}{L} & 0 \\ 0 & \frac{-R}{L} \end{bmatrix}\begin{bmatrix} I_{\alpha p} \\ I_{\beta p} \end{bmatrix} + \begin{bmatrix} \frac{1}{L} & 0 \\ 0 & \frac{1}{L} \end{bmatrix}\begin{bmatrix} V_{\alpha p} \\ V_{\beta p} \end{bmatrix} - \begin{bmatrix} \frac{1}{L} & 0 \\ 0 & \frac{1}{L} \end{bmatrix}\begin{bmatrix} e_{\alpha p} \\ e_{\beta p} \end{bmatrix}. \tag{7}$$

- Secondary machine:

$$\frac{d}{dt}\begin{bmatrix} I_{\alpha s} \\ I_{\beta s} \end{bmatrix} = \begin{bmatrix} \frac{-R}{L} & 0 \\ 0 & \frac{-R}{L} \end{bmatrix}\begin{bmatrix} I_{\alpha s} \\ I_{\beta s} \end{bmatrix} + \begin{bmatrix} \frac{1}{L} & 0 \\ 0 & \frac{1}{L} \end{bmatrix}\begin{bmatrix} V_{\alpha s} \\ V_{\beta s} \end{bmatrix} - \begin{bmatrix} \frac{1}{L} & 0 \\ 0 & \frac{1}{L} \end{bmatrix}\begin{bmatrix} e_{\alpha s} \\ e_{\beta s} \end{bmatrix}. \tag{8}$$

3.2. Modeling of the five-phase inverter

Figure 2 shows the structure of a five-phase inverter. Each arm of the inverter can be presented by a two-position switch.

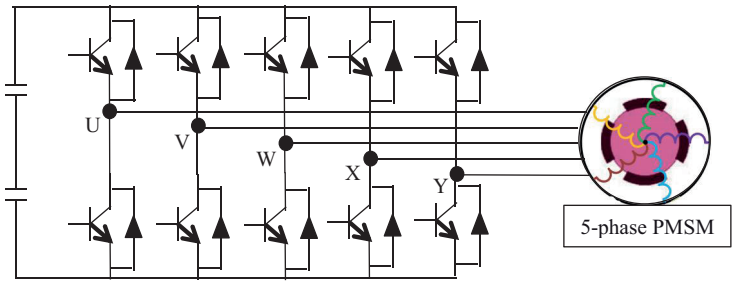

Figure 2. Example of a five-phase inverter for the five-phase synchronous machine.

The inverter switches are considered ideal. The states of the switches are represented by a vector of dimension (5 * 1) given by:

$$[S] = \begin{bmatrix} S_a \\ S_b \\ S_c \\ S_d \\ S_e \end{bmatrix}. \tag{9}$$

The phase voltages as a function of the conduction state of the inverter are expressed as:

$$[V] = \begin{bmatrix} V_a \\ V_b \\ V_c \\ V_d \\ V_e \end{bmatrix} = \frac{V_0}{5} \begin{bmatrix} 4 & -1 & -1 & -1 & -1 \\ -1 & 4 & -1 & -1 & -1 \\ -1 & -1 & 4 & -1 & -1 \\ -1 & -1 & -1 & 4 & -1 \\ -1 & -1 & -1 & -1 & 4 \end{bmatrix} [S]. \tag{10}$$

Combinations of the 5 quantities (S_a, S_b, S_c, S_d, and S_e) permit generating 32 vector positions [V] since 2 corresponds to the zero vectors: (S_a, S_b, S_c, S_d, and S_e)=(00000) or (11111).

The projections of stator voltage vectors in each imaginary plane under consideration are shown in Figures 3 and 4 [6].

The vectors v_0 and v_{31} have a zero projection in the two considered planes. There are three groups, each of them is composed of 10 distinct vectors. The first group is composed of 10 vectors that represent the upper decagon in the principal plane and the lower decagon in the secondary plane. The second group is composed of 10 vectors that represent the lower decagon in the principal plane and the upper decagon in the secondary plane. The third group is composed of 10 vectors which represent the intermediate decagon in each of the two considered planes [39].

In the Concordia landmark, the voltage vector [V] in each fictitious plane is given by:

$$\begin{bmatrix} V_{\alpha p} \\ V_{\beta p} \end{bmatrix} = [C_p] \frac{V_0}{5} \begin{bmatrix} 4 & -1 & -1 & -1 & -1 \\ -1 & 4 & -1 & -1 & -1 \\ -1 & -1 & 4 & -1 & -1 \\ -1 & -1 & -1 & 4 & -1 \\ -1 & -1 & -1 & -1 & 4 \end{bmatrix} [S], \tag{11}$$

$$\begin{bmatrix} V_{\alpha s} \\ V_{\beta s} \end{bmatrix} = [C_s]\frac{V_0}{5}\begin{bmatrix} 4 & -1 & -1 & -1 & -1 \\ -1 & 4 & -1 & -1 & -1 \\ -1 & -1 & 4 & -1 & -1 \\ -1 & -1 & -1 & 4 & -1 \\ -1 & -1 & -1 & -1 & 4 \end{bmatrix}[S]. \tag{12}$$

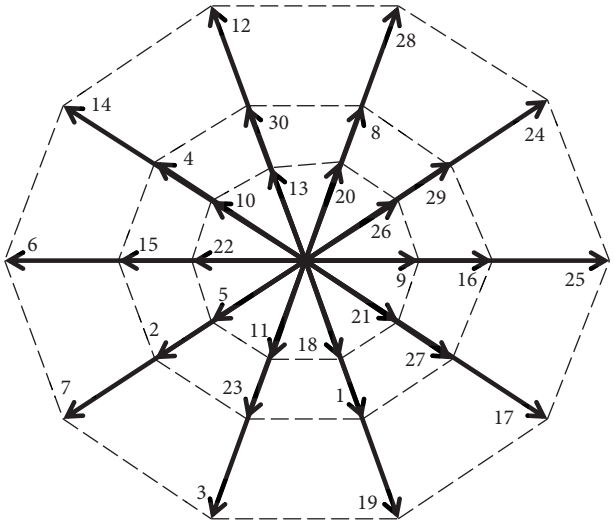

Figure 3. The projection of the voltage vectors in the main plane.

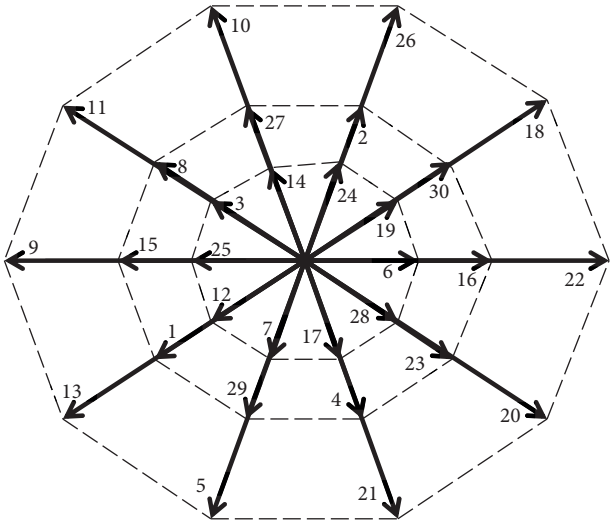

Figure 4. The projection of the voltage vectors in the secondary plane.

4. Algorithm of the proposed control

For a five-phase permanent-magnet synchronous machine with smooth poles, the electromagnetic torque can be expressed as:

$$T_{em} = p\sqrt{\frac{5}{2}}[\phi_{fP} i_{qp} + 3\phi_{fs} i_{qs}]. \tag{13}$$

In the case of machines with sinusoidal flow distribution, only the first fictitious machine M1 produces an electromotive force (FEM) voltage [39–41]. Thus, it is the only one to produce an electromagnetic torque.

$$T_{em} = p\sqrt{\frac{5}{2}}[\phi_{fP} i_{qp}]. \tag{14}$$

In this case, the inverter uses only the vectors v_0 and v_{31} that have a null projection and the group 1 of 10 vectors of the same standard which represents the upper decagon in the main plane.

The electromagnetic torque is proportional to the current i_{qp}. In the state space, the current references are therefore i_{dpref}=0 (to minimize Joule losses) and i_{qpref} proportional to the torque setpoint [23, 24].

The algorithm of control uses a technique of calculation of the switching. The latter is based on the vector representation of the current vectors in the plane (α, β); the reference currents i_{dref} and i_{qref} must then be transformed into two sinusoidal currents $i_{\alpha ref}$ and $i_{\beta ref}$, and then calculate the reference direction d_{ref}.

This algorithm of control consists of projecting the desired vector d_{ref} on the two adjacent direction vectors that correspond to two switching states of the inverter during a period T. The operation of the studied control is summarized by the following processing sequences:

- Obtaining a hybrid model of the combined converter-machine.
- Calculating the possible directions in the state space.
- Acquiring a setpoint d_{ref}.
- Determining the sector containing the vector d_{ref}.
- Decomposing the vector d_{ref} following the two vectors d_i and d_{i+1} delimiting the sector i.
- Elaborating the control sequences of the inverter switches.

4.1. Hybrid model of the behavior of the inverter-machine combined

Starting from Eqs. (7) and (11), the hybrid model of the behavior of the inverter-machine set is written:

$$\frac{d}{dt}\begin{bmatrix} I_{\alpha p} \\ I_{\beta p} \end{bmatrix} = \begin{bmatrix} \frac{-R}{L} & 0 \\ 0 & \frac{-R}{L} \end{bmatrix} \begin{bmatrix} I_{\alpha p} \\ I_{\beta p} \end{bmatrix} + \begin{bmatrix} \frac{1}{L} & 0 \\ 0 & \frac{1}{L} \end{bmatrix} [C_p] \frac{V_0}{5} \begin{bmatrix} 4 & -1 & -1 & -1 & -1 \\ -1 & 4 & -1 & -1 & -1 \\ -1 & -1 & 4 & -1 & -1 \\ -1 & -1 & -1 & 4 & -1 \\ -1 & -1 & -1 & -1 & 4 \end{bmatrix} [S] - \begin{bmatrix} \frac{1}{L} & 0 \\ 0 & \frac{1}{L} \end{bmatrix} \begin{bmatrix} e_{\alpha p} \\ e_{\beta p} \end{bmatrix}. \tag{15}$$

The integration of Eq. (11) by the Euler method over a short time interval T gives:

$$\begin{bmatrix} I_{\alpha p}(k+1) \\ I_{\beta p}(k+1) \end{bmatrix} = \begin{bmatrix} 1-\frac{TR}{L} & 0 \\ 0 & 1-\frac{TR}{L} \end{bmatrix} \begin{bmatrix} I_{\alpha p}(k) \\ I_{\beta p(k)} \end{bmatrix} + \begin{bmatrix} \frac{T}{L} & 0 \\ 0 & \frac{T}{L} \end{bmatrix} [C_p] \frac{V_0}{5} \begin{bmatrix} 4 & -1 & -1 & -1 & -1 \\ -1 & 4 & -1 & -1 & -1 \\ -1 & -1 & 4 & -1 & -1 \\ -1 & -1 & -1 & 4 & -1 \\ -1 & -1 & -1 & -1 & 4 \end{bmatrix} [S] - \begin{bmatrix} \frac{T}{L} & 0 \\ 0 & \frac{T}{L} \end{bmatrix} \begin{bmatrix} e_{\alpha p} \\ e_{\beta p} \end{bmatrix}. \tag{16}$$

Taking:

$$A = \begin{bmatrix} 1-\frac{TR}{L} & 0 \\ 0 & 1-\frac{TR}{L} \end{bmatrix}, \tag{17}$$

$$d_j = \begin{bmatrix} \frac{T}{L} & 0 \\ 0 & \frac{T}{L} \end{bmatrix} [C_p] \frac{V_0}{5} \begin{bmatrix} 4 & -1 & -1 & -1 & -1 \\ -1 & 4 & -1 & -1 & -1 \\ -1 & -1 & 4 & -1 & -1 \\ -1 & -1 & -1 & 4 & -1 \\ -1 & -1 & -1 & -1 & 4 \end{bmatrix} [S], \tag{18}$$

$$D = -\begin{bmatrix} \frac{T}{L} & 0 \\ 0 & \frac{T}{L} \end{bmatrix} \begin{bmatrix} e_{\alpha p} \\ e_{\beta p} \end{bmatrix}. \tag{19}$$

So the hybrid model of our system is written in the following form:

$$\begin{bmatrix} I_{\alpha p}(k+1) \\ I_{\beta p}(k+1) \end{bmatrix} = A \begin{bmatrix} I_{\alpha p}(k) \\ I_{\beta p}(k) \end{bmatrix} + d_j + D. \tag{20}$$

4.2. Determination of directions

For a measured state, the algorithm of control computes the possible evolutions in the state space relating to the different configurations, using Eq. (20). A graphical representation of these vectors is given in Figure 5.

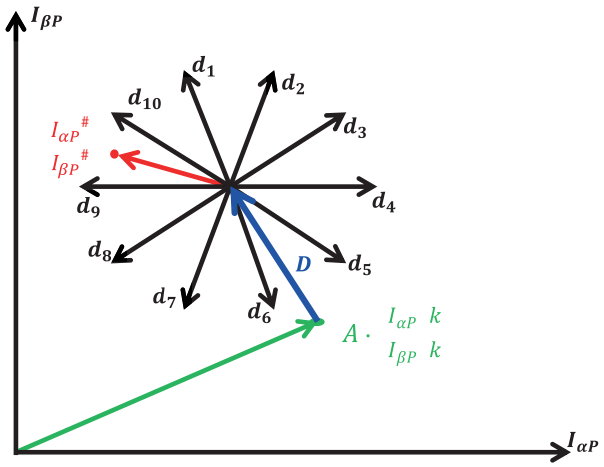

Figure 5. Example of possible directions in the plane (I_α, I_β).

Starting from Figure 5, the possible directions and reference direction are given as follows:

$$d_j = \begin{bmatrix} I_{\alpha p}(k+1) \\ I_{\beta p}(k+1) \end{bmatrix} - A \begin{bmatrix} I_{\alpha p}(k) \\ I_{\beta p}(k) \end{bmatrix} - D, \tag{21}$$

$$d_{ref} = \begin{bmatrix} I_{\alpha pref} \\ I_{\beta pref} \end{bmatrix} - A \begin{bmatrix} I_{\alpha p}(k) \\ I_{\beta p}(k) \end{bmatrix} - D. \tag{22}$$

4.3. Determination of the sector

In order to determine the sector to which the reference vector d_{ref} belongs, we must determine the integer i $(1 \leq i \leq 10)$.

Taking:

$$\Theta_{ref} = \begin{cases} arg(d_{ref}) & \text{if} \quad arg(d_{ref}) \geq 0 \\ arg(d_{ref}) + 2\pi & \text{if} \quad arg(d_{ref}) < 0 \end{cases} \tag{23}$$

It is then possible to determine the sector i by the following relation:

$$i = \sum_{m=1}^{10} mF(\Theta_{ref} - (m-1)\frac{2\pi}{5}), \tag{24}$$

where F is a function that takes the following values:

$$F(\Theta) = \begin{cases} 1 & \text{if} \quad 0 \leq \theta \leq \frac{2\pi}{5} \\ 0 & \text{if} \quad NO \end{cases} \tag{25}$$

4.4. Calculation of t_i and t_{i+1} for each sector

To obtain a vector closer to the desired direction, it is necessary to apply:

- The voltage v_i corresponding to the vector d_i during the time t_i;
- The voltage v_{i+1} corresponding to the vector d_{i+1} during the time t_{i+1};
- A null vector during times t_0 and t_{31}.

With the time durations t_0 and t_{31} defined by the following relation:

$$t_0 + t_{31} = T - t_i - t_{i+1}, \tag{26}$$

the equation of the reference vector becomes:

$$d_{ref} = \frac{d_i t_i}{T} + \frac{d_{i+1} t_{i+1}}{T}. \tag{27}$$

We can deduce the relations that allow calculating the switching time for the different sectors:

$$\begin{cases} t_i = \frac{|d_{ref}| T sin(\frac{i\pi}{5} - \Theta_{ref})}{|d| sin(\frac{\pi}{5})} \\ t_{i+1} = \frac{|d_{ref}| T sin(\Theta_{ref} - \frac{(i-1)\pi}{5})}{|d| sin(\frac{\pi}{5})} \\ t_0 = t_{31} = \frac{T - t_i - t_{i+1}}{2} \end{cases} \tag{28}$$

5. Simulation results and interpretation

The operation of the inverter-machine unit was simulated using MATLAB/Simulink software. Two cases are to be realized: the hybrid control and the classical vector control.

To verify the performance of the studied control, it is necessary to make a comparison between the two orders made under the same operating conditions and in the same simulation configuration. In terms of:

- Better static and dynamic performance
- Best application of the control instructions
- Better releases of disturbances
- Insensitivity to parameter variations

The machine used has the following characteristics: Rs=0.12 Ω; Ld=Lq=1.35mH; ϕ_f =0.05 Wb; p=4

The global model is presented in Figure 6.

Figures 7–10 shows the obtained results in steady state with the two controls (vector control and hybrid control) for a reference i_{sqref} equal to the nominal current (i_{sqref} =5A) and a reference i_{sdref} null. These results show the obtained patterns of the currents i_{sd} et i_{sq}, electromagnetic torque and phase currents.

From the results obtained, we can say that the two controllers demonstrate good prosecutions. However, it is interesting to note that the hybrid controller is able to reduce the current ripple i_{sq} and torque. In Figure 10 the phase currents for the two controls have the appearance of sinusoid with a low noise in the case of the hybrid

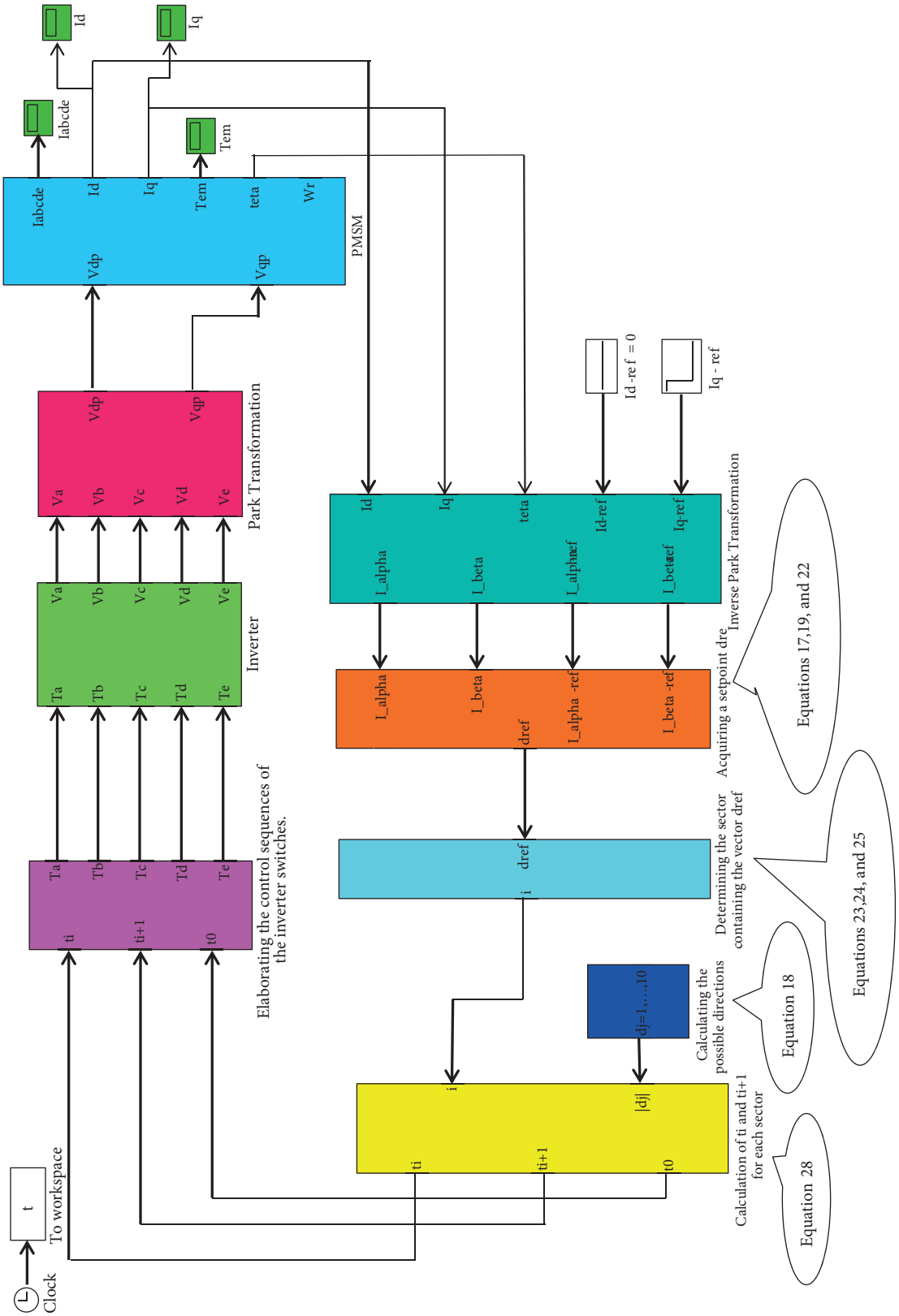

Figure 6. Simulation scheme of hybrid control.

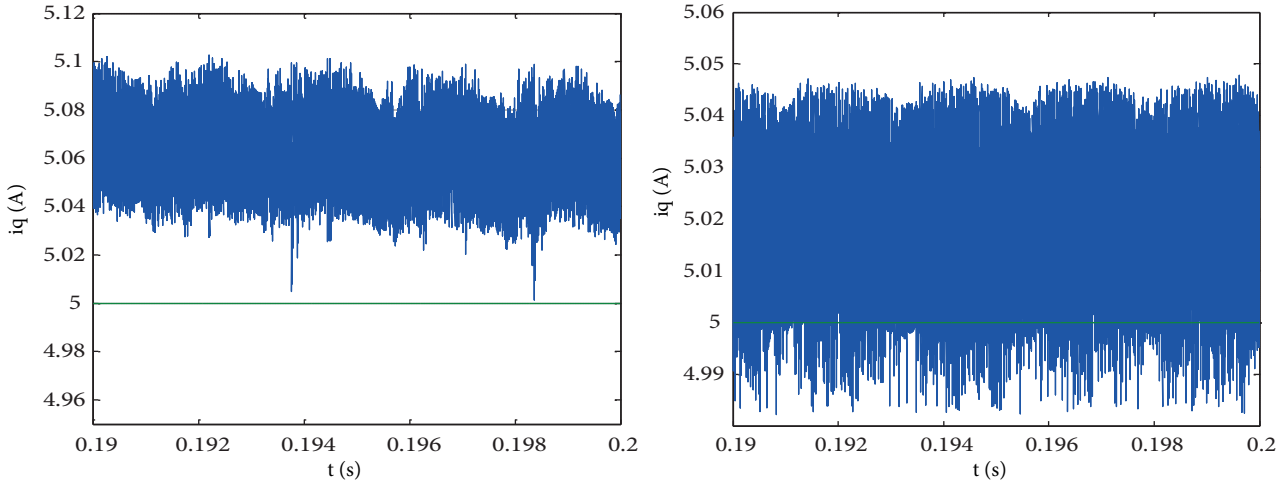

Figure 7. The obtained steady-state current i_{sq} in the case of (Left) vector control, (Right) hybrid control.

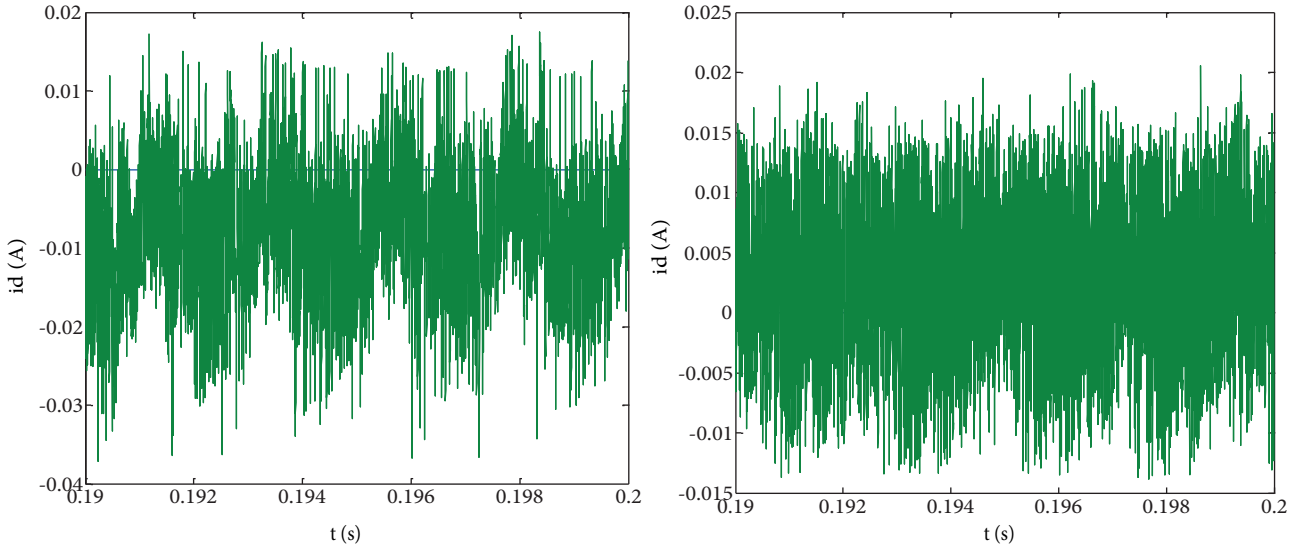

Figure 8. The obtained steady-state current i_{sd} in the case of (Left) vector control, (Right) hybrid control.

control. This remark can be confirmed by the spectra of the phase currents shown in Figure 11, when using the hybrid control; all harmonics have disappeared.

To further test the robustness of the control with respect to a reference variation of the current i_{sq}, a change in the current setpoint of +5 to –5 is introduced at the instant t = 0.05 s.

Figures 12 and 13 shows the currents in the marks (d, q). The current setpoint Isq is reached in 200 μs for hybrid control against 700 μs for vector control. With the hybrid control, we can see the steady hold of Isd during the abrupt change of the current reference i_{sq}. Concerning the vector control, one can note the effect of recoupling on the current Isd during this change, which induces a slower response time.

In Figure 14, it is noticeable that the control of the currents by the hybrid control during switching of the converter does not lead to any overcurrent, contrary to the classical vector control where the current exceeds the set value.

Figure 15 shows the responses of the torque for the two control. The comparison of these results shows

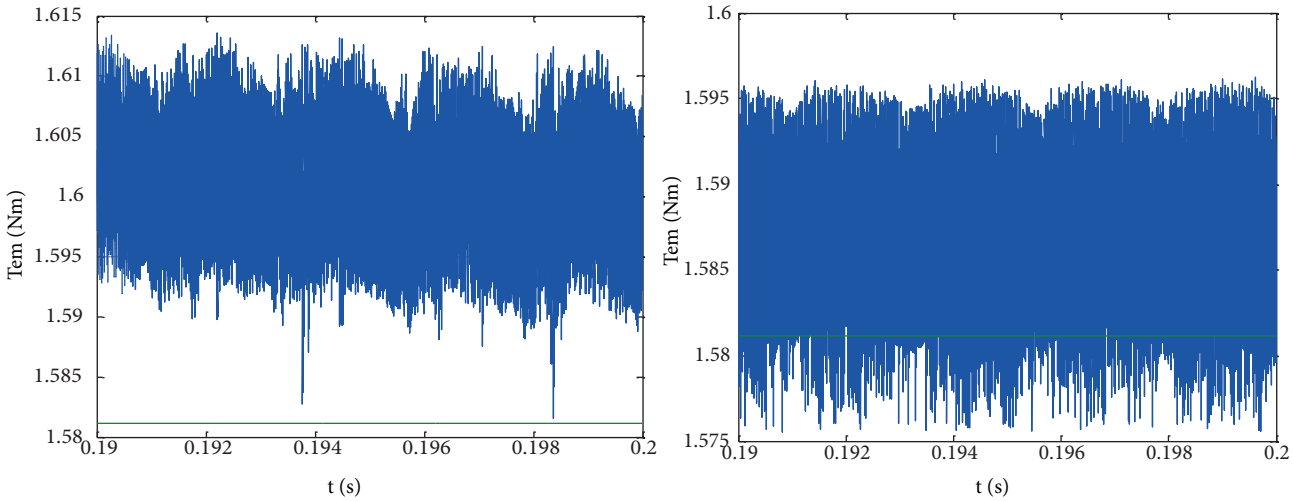

Figure 9. The obtained steady-state torque in the case of (Left) vector control, (Right) hybrid control.

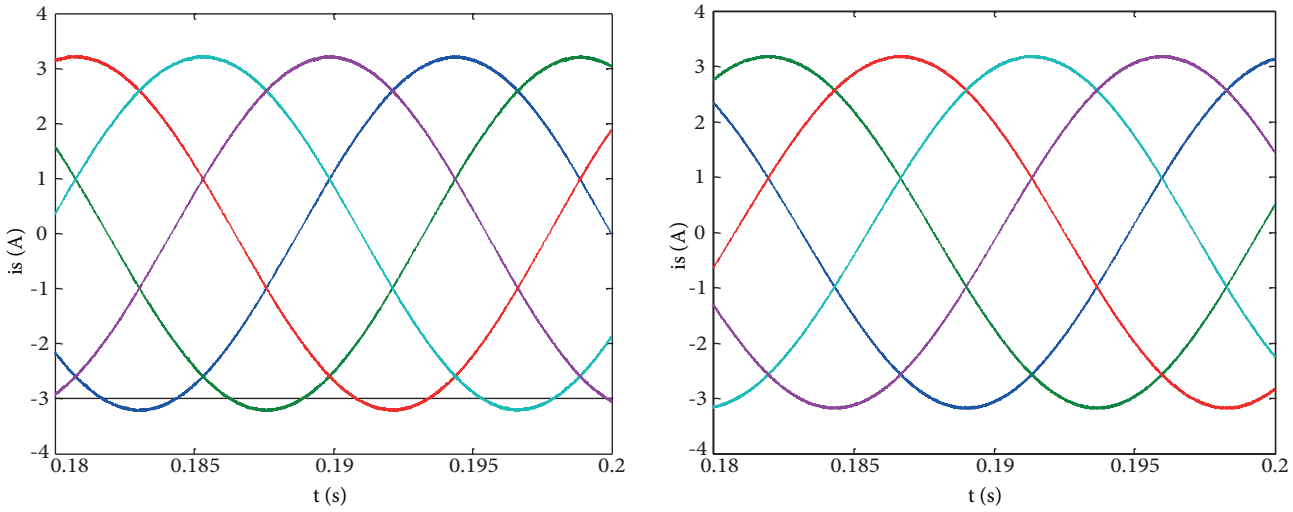

Figure 10. The obtained steady-state currents of phases in the case of (Left) vector control, (Right) hybrid control.

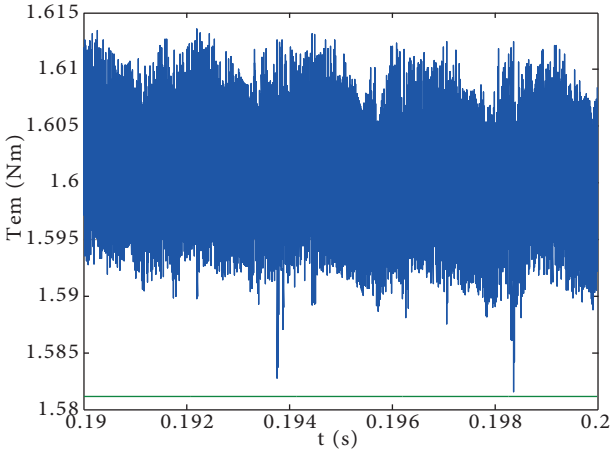

Figure 11. The Phase current harmonic spectrum in the case of (Left) vector control, (Right) hybrid control.

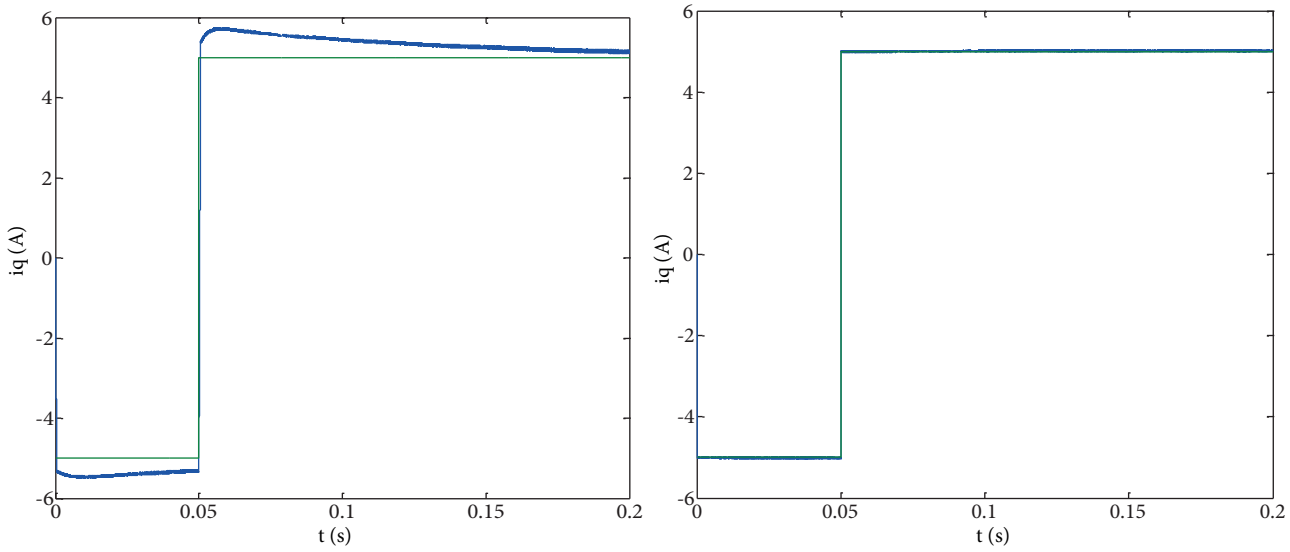

Figure 12. The obtained transient-state current i_{sq} in the case of (Left) vector control, (Right) hybrid control.

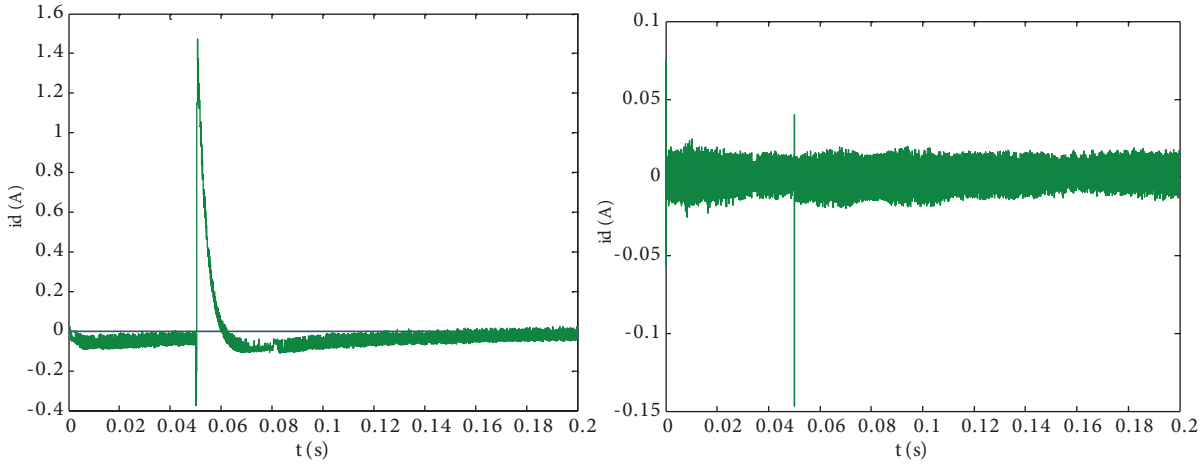

Figure 13. The obtained transient-state current i_{sd} in the case of (Left) vector control, (Right) hybrid control.

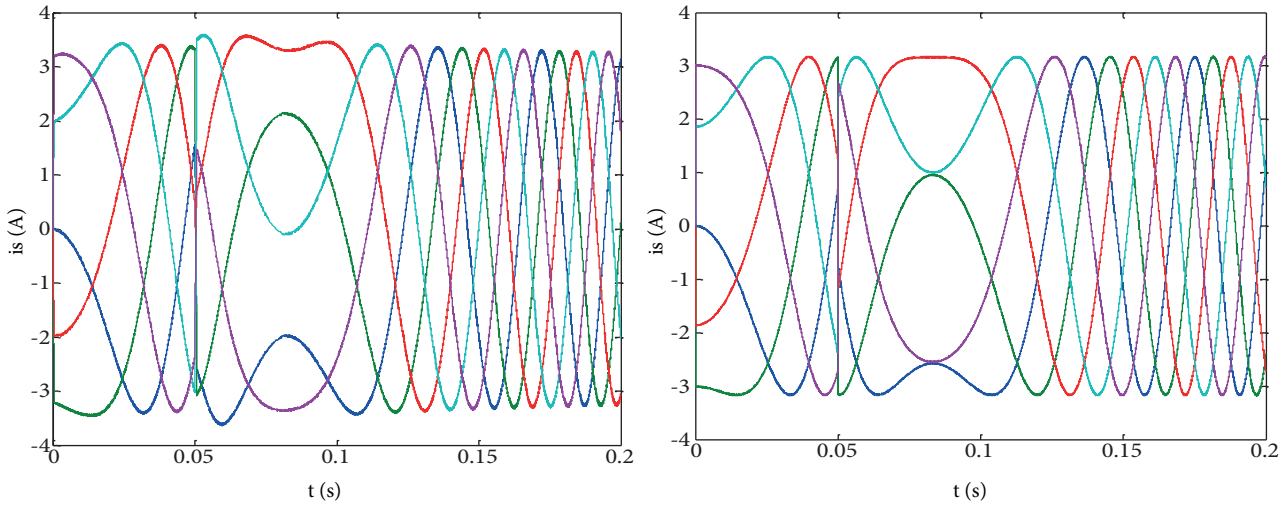

Figure 14. The obtained transient-state currents of phases in the case of (Left) vector control, (Right) hybrid control.

that the hybrid control shows very high dynamics and precision of response of the torque, contrary to the classical vector control. In order to have a better appreciation of the obtained results through the two commands, we have represented the couple in Figure 16.

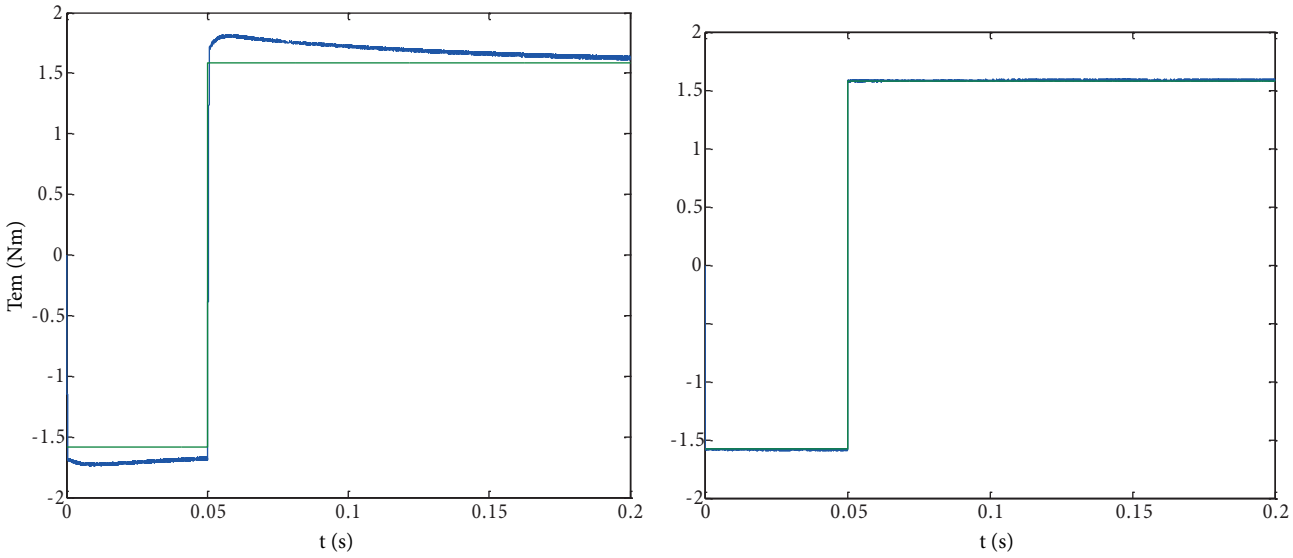

Figure 15. The obtained transient-state torque in the case of (Left) vector control, (Right) hybrid control.

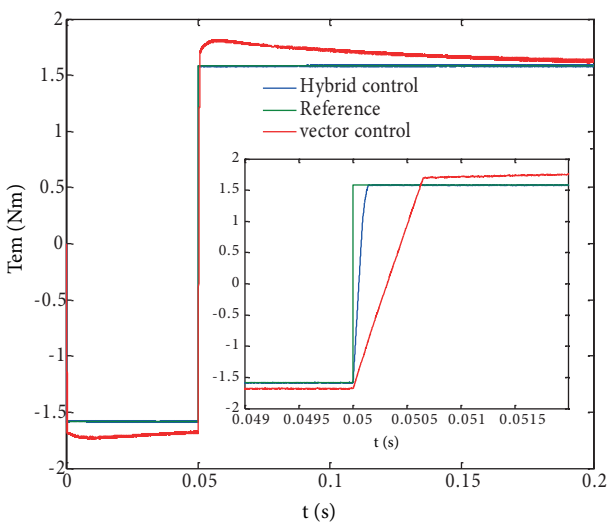

Figure 16. The obtained transient-state torque evolution for both controls.

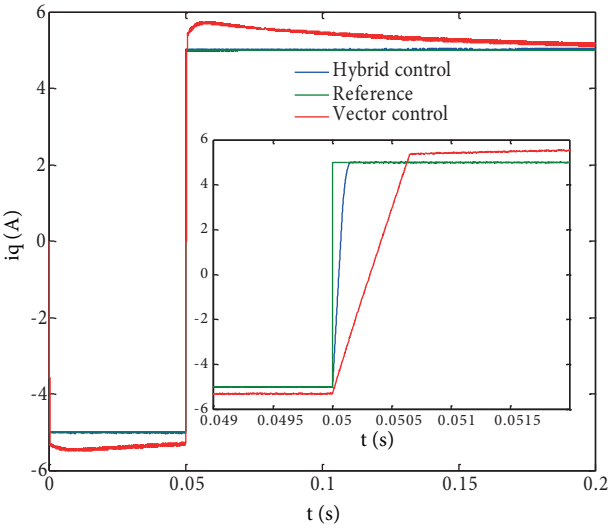

Figure 17. The obtained transient-state current i_{sq} evolution for both controls.

Figure 18 shows the comparison between the influence of the variation of the parameters that characterize the model on the performances of the vector control and that of the hybrid control in order to evaluate the robustness of the latter.

For this purpose, the value of the stator resistance and the value of the inductance are increased +100% of their nominal values in the model of the machine only, keeping these nominal values in the control algorithm. And the response of the components i_{sd} and i_{sq} and the torque response are presented when applying steps to the reference i_{sqref} of +5 to –5 while maintaining the reference i_{sdref} null.

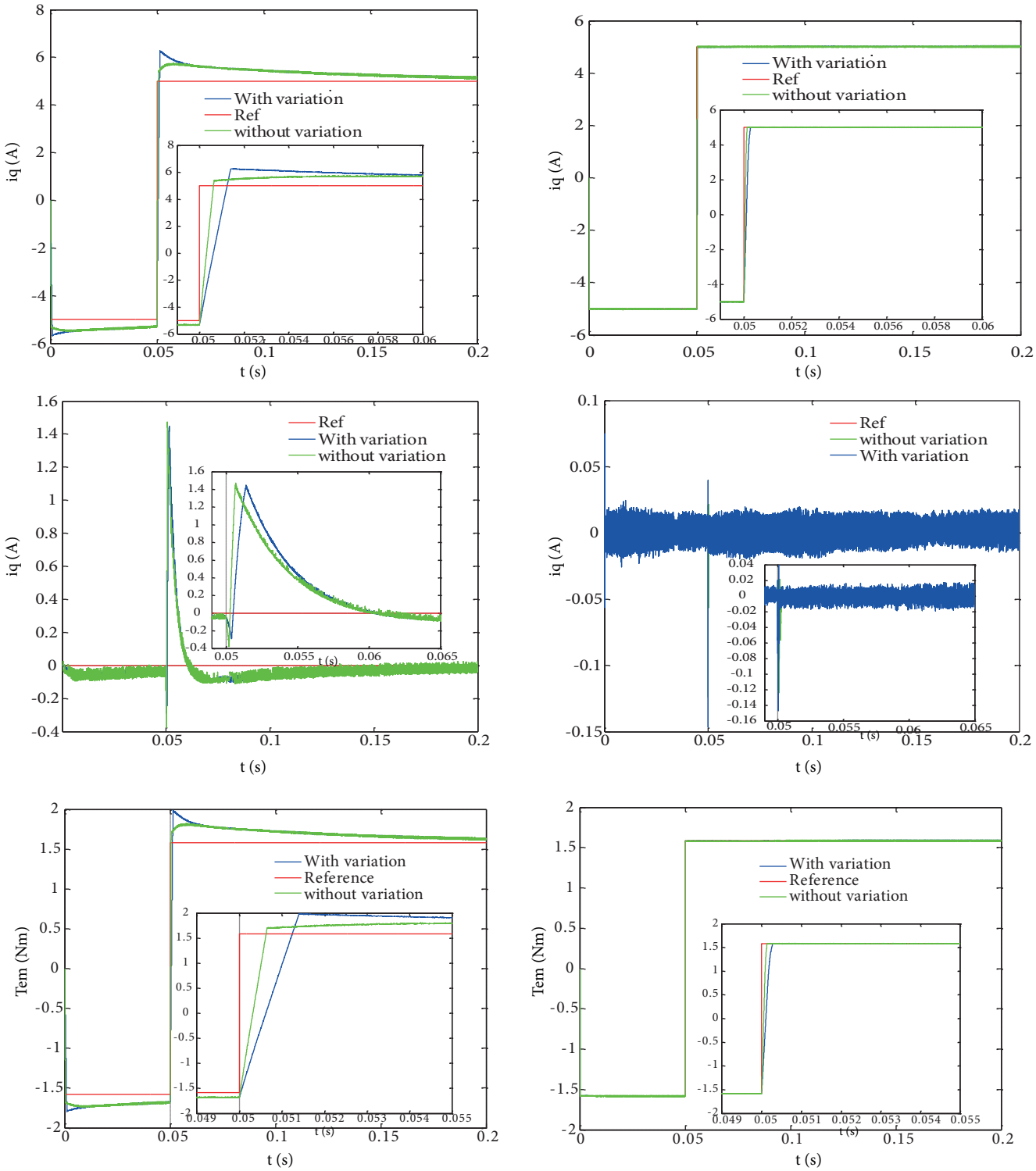

Figure 18. Simulation results during variations of the machine parameters.

From Figure 18, it is found that the vector control law depends on the parameters of the motor; therefore, this technique is not robust regarding the internal parametric variations. However, in the hybrid control, it was observed that the parameters of the control algorithm are less dependent on the parameters of the machine.

6. Conclusion

In this paper, we have studied the hybrid control of five-phase permanent-magnet synchronous machine associated with the SVM technique. Thanks to this control strategy, the operation of the system can be improved. This technique is based on a very simple local model valid for a time horizon of decision. This reduces the complexity of the algorithm and it is noted that this control does not need any observers or current regulators.

The model was established on MATLAB/SIMULINK. Simulation results are presented to demonstrate the validity of this model. These results showed very good dynamic performance and good robustness with respect to the parametric variations that would be impossible to obtain by the conventional approaches.

References

[1] Arahal MR, Barrero F, Toral S, Duran M, Gregor R. Multi-phase current control using finite-state model-predictive control. Control Engineering Practice 2009; 17: 579-587.

[2] Iqbal A, Singh GK, Pant V. Some observations on no-load losses of an asymmetrical six-phase synchronous machine. Turk J Elec Eng & Comp Sci 2016; 24: 4497-4507.

[3] Abjadi NR. Sliding-mode control of a six-phase series/parallel connected two induction motors drive. ISA Transactions 2014; 53: 1847-1856.

[4] Hosseyni A, Trabelsi R, Mimouni MF, Iqbal A, Alammari R. Sensorless sliding mode observer for a five-phase permanent magnet synchronous motor drive. ISA Transactions 2015; 58: 462-473.

[5] Iqbal A, Singh GK, Pant V. Stability analysis of an asymmetrical six-phase synchronous motor. Turk J Elec Eng & Comp Sci 2016; 24: 1674-1692.

[6] Barik SK, Jaladi KK. Five-phase induction motor DTC-SVM scheme with PI controller and ANN controller. Procedia Technology 2016; 25: 816-823

[7] Wang X, Wang Z, Xu Z. A hybrid direct torque control scheme for dual three-phase PMSM drives with improved operation performance. IEEE Transactions on Power Electronics 2018; 63: 321-333.

[8] Echeikh H, Trabelsi R, Iqbal A, Bianchi N, Mimouni MF. Non-linear control of five-phase IM drive at low speed conditions–experimental implementation. ISA Transactions 2016; 65: 244-253

[9] Bermudez M, Gomozov O, Kestelyn X, Barrero F, Nguyen NK, Semail E. Model predictive optimal control considering current and voltage limitations: real-time validation using OPAL-RT technologies and five-phase permanent magnet synchronous machines. Mathematics and Computers in Simulation 2018; 63: 321-333.

[10] Hosseyni A, Trabelsi R, Iqbal A, Mimouni MF. Comparative study of adaptive sliding mode and resonant controllers in fault tolerant five-phase permanent magnet synchronous motor drive. The International Journal of Advanced Manufacturing Technology 2018; 96: 2195-2213.

[11] Arahal MR, Barrero F, Durán MJ, Ortega MG, Martín C. Trade-offs analysis in predictive current control of multi-phase induction machines. Control Engineering Practice 2018; 81: 105-113.

[12] Semail E. Multi-phase electrical drives: Towards a System Approach. Report of the Habilitation to Directing Researches, Lille University of Science and Technologie, Lille, France, 2009.

[13] Crévits Y. Characterization and control of multiphase drives under fault supply conditions. PhD thesis, University of Lille, Lille, France, 2010.

[14] Khedher A, Mimouni MF. Sensorless-adaptive DTC of double star induction motor. Energy Conversion and Management 2010; 51: 2878-2892.

[15] Arahal MR, Duran MJ. PI tuning of five-phase drives with third harmonic injection. Control Engineering Practice 2009; 17: 787-797.

[16] Boudjema Z, Taleb R, Djeriri Y, Yahdou A. A novel direct torque control using second order continuous sliding mode of a doubly fed induction generator for a wind energy conversion system. Turk J Elec Eng & Comp Sci 2017; 25: 965-975.

[17] Ouassaid M, Elyaalaoui K, Cherkaoui M. Sliding mode control of induction generator wind turbine connected to the grid. Advances and Applications in Nonlinear Control Systems 2016; 635:531-553

[18] Monmasson E, Louis JP. Presentation of a control law for IM drive based on the dynamic reconfiguration of a DTC algorithm and a SVM-DTC algorithm. Mathematics and Computers in Simulation 2003; 63: 321-333.

[19] Ammar A, Benakcha A, Bourek A. Closed loop torque SVM-DTC based on robust super twisting speed controller for induction motor drive with efficiency optimization. International Journal of Hydrogen Energy 2017; 42: 17940-17952

[20] Pimkumwong N, Wang MS. Full-order observer for direct torque control of induction motor based on constant V/F control technique. ISA Transactions 2018; 73: 189-200.

[21] Mesloub H, Boumaaraf R, Benchouia MT, Goléa A, Goléa N, Srairi K. Comparative study of conventional DTC and DTC SVM based control of PMSM motor - simulation and experimental results. Mathematics and Computers in Simulation 2018; 63: 321–333.

[22] Morel F, Retif JM, Lin-Shi X, Valentin C. Permanent magnet synchronous machine hybrid torque control. IEEE transactions on industrial electronics 2008; 55: 501-511.

[23] Lin-Shi X, Morel F, Llor A, Allard B, Rétif JM. Implementation of hybrid control for motor drives. IEEE Transactions on Ind Electronis 2007; 54: 1946-1952.

[24] Lin-Shi X . Control of energy conversion systems. Habilitation to Directing Researches. National Institution of Applied Sciences of Lyon, Lyon, France 2007.

[25] Morel F, Lin-Shi X, Rétif JM, Allard B.A predictive current control applied to a permanent magnet synchronous machine, comparison with a classical direct torque control. Electric Power Systems 2008; 78: 1437-1447.

[26] Retif JM, Lin-Shi X, Llor AM, Morand F. New hybrid direct-torque control for a winding rotor synchronous machine. In: IEEE 2004 Power Electronics Specialists Conference; 20-25 June 2004 ; Aachen, Germany, Germany : IEEE. pp. 1438-1442

[27] Morel F, Rtif JM, Lin-Shi X, LIor AM. Fixed switching frequency hybrid control for a permanent magnet synchronous machine. In: IEEE 2004 International Conference on Industrial Technology; 8-10 Dec 2004 ; Hammamet, Tunisia, Tunisia : IEEE. pp. 127-131

[28] Arichi F, Gorp JV, Djemai M, Defoort M, Cherki B. Hybrid state estimation for a class of switched system using Petri Nets. In: IEEE 2014 European Control Conference; 24-27 June 2014; Strasbourg, France: IEEE. pp. 2534-2539

[29] Elmetennani S, Laleg-Kirati TM, Djemai M, Tadjine M. New MPPT algorithm for PV applications based on hybrid dynamical approach. Journal of Process Control 2016; 48: 14-24.

[30] Gorp JV, Giua A, Defoort M, Djemaï M. Active diagnosis for switched systems using mealy machine modeling. In: Sayed-Mouchaweh M, editor. Diagnosability, Security and Safety of Hybrid Dynamic and Cyber-Physical Systems. New York, NY, USA : Springer International Publishing, 2018. pp. 147-173

[31] Djondiné P, Barbot JP, Ghanes M. On the Petri nets control of the multicellular converter. International Journal of Emerging Technology and Advanced Engineering 2017; 7: 332-336.

[32] Liu X, Stechlinski P. Switching and impulsive control algorithms for nonlinear hybrid dynamical systems. Nonlinear Analysis: Hybrid Systems 2018; 27: 307–322.

[33] Halbaoui K, Belazreg MF, Boukhetala D, Belhouchat MH. Modeling and predictive control of nonlinear hybrid systems using mixed logical dynamical formalism. In: Vaidyanathan S, Volos C, editors. Advances and Applications in Nonlinear Control Systems. New York, NY, USA : Springer International Publishing, 2016. pp. 421-450

[34] Djondiné P, Barbot JP, Ghanes M. Comparison of sliding mode and petri nets control for multicellular chopper. International Journal of Nonlinear Science 2018; 25: 67-75.

[35] Defoort M, Gorp JV, Djemai M. Multicellular converter: a benchmark for control and observation for hybrid dynamical systems. In: Djemai M, Defoort M, Editors. Hybrid Dynamical Systems. New York, NY, USA : Springer International Publishing, 2015. pp. 293-313

[36] Benmiloud M, Benalia A. Hybrid control scheme for multicellular converter. In: IEEE 2013 International Conference on Control, Decision and Information Technologies (CoDIT); 6-8 May 2013; Hammamet, Tunisia : IEEE. pp. 476-482.

[37] Benmansour K, Benalia A, Djemai M, Leon J. Hybrid control of a multicellular converter. Nonlinear Analysis: Hybrid Systems 2007; 1: 16–29.

[38] Sellam A, Dehiba B, Benabdallah MB, Abid M, Bouiadjra NB, Bensaid B, Djouhri M. A vectorial modeling for the permanent magnet synchronous machine polyphase based on multimachine approach. International Journal on Electrical Engineering and Informatics 2013; 5: 67-80

[39] Jones M, Satiawan INW. A simple multi-level space vector modulation algorithm for five-phase open-end winding drives. Mathematics and Computers in Simulation 2013: 90: 74–85

[40] Toliyat, HA. Analysis and simulation of multi-phase variable speed induction motor drives under asymmetrical connections. In: IEEE 1996 Applied Power Electronics Conference and Exposition; 3-7 March 1996; San Jose, CA, USA: IEEE. pp. 586-592.

[41] Vizireanu D, Brisset S, Kestelyn X, Brochet P, Miletet Y, Laloy D. Investigation on multi-star structures for large power direct-drive wind generator. Electric Power Components and Systems 2007; 35: 135-152.